Icarus 217 (2012) 856–862

Contents lists available at ScienceDirect

Icarus

journal homepage: www.elsevier.com/locate/icarus

# Thermospheric/mesospheric temperatures on Venus: Results from ground-based high-resolution spectroscopy of $CO_2$ in 1990/1991 and comparison to results from 2009 and between other techniques

Guido Sonnabend [a,*], Peter Krötz [a], Frank Schmülling [b,c], Theodor Kostiuk [b,1], Jeff Goldstein [d,1], Manuela Sornig [f], Dušan Stupar [a], Timothy Livengood [d], Tilak Hewagama [e], Kelly Fast [b], Arnaud Mahieux [g]

[a] Physikalisches Institut, Universität zu Köln, Zülpicher Str. 77, 50937 Köln, Germany
[b] NASA GSFC, Code 693, MD 20771, USA
[c] DLR, Königswintererstr. 522, 53227 Bonn, Germany
[d] NCESSE, P.O. Box 3806, Capitol Heights, MD 20791, USA
[e] University of Maryland, College Park, MD 20742, USA
[f] Rheinisches Institut fuer Umweltforschung, Abt. Planetenforschung, 50931 Köln, Germany
[g] Belgian Institute for Space Aeronomy, Avenue Circulaire 3, 1180 Brussels, Belgium

ARTICLE INFO

*Article history:*
Available online 23 July 2011

*Keywords:*
Venus, Atmosphere
Infrared observations
Spectroscopy

ABSTRACT

We report temperatures in Venus' upper mesosphere/lower thermosphere, deduced from reanalyzing very high resolution infrared spectroscopy of $CO_2$ emission lines acquired in 1990 and 1991. Kinetic temperatures at ~110 km altitude (0.15 Pa) are derived from the Doppler width of fully-resolved single line profiles measured near 10.4 μm wavelength using the NASA GSFC Infrared Heterodyne Spectrometer (IRHS) at the NASA IRTF on Mauna Kea, HI, close to Venus inferior conjunction and two Venus solstices. Measured temperatures range from ~200 to 240 K with uncertainty typically less than 10 K. Temperatures retrieved from similar measurement in 2009 using the Cologne Tuneable Heterodyne Infrared Spectrometer (THIS) at the NOAO McMath Telescope at Kitt Peak, AZ are 10–20 K lower. Temperatures retrieved more recently from the SOIR instrument on Venus EXpress are consistent with these results when the geometry of observation is accounted for. It is difficult to compare ground-based sub-mm retrievals extrapolated to 110 km due to their much larger field of view, which includes the night side regions not accessible to infrared heterodyne observations. Temperature variability appears to be high on day-to-day as well as longer timescales. Observed short term and long term variability may be attributed to atmospheric dynamics, diurnal variability and changes over solar activity and seasons. The Venus International Reference Atmosphere (VIRA) model predicts cooler temperatures at the sampled altitudes in the lower thermosphere/upper mesosphere and is not consistent with these measurements.

© 2011 Elsevier Inc. All rights reserved.

## 1. Introduction

Recent results from Venus EXpress (VEX) has renewed interest in Venus' atmosphere. Observations since the arrival of VEX in 2006 showed that the Venus International Reference Atmosphere (VIRA) model (Keating et al., 1985; Seiff et al., 1985) which was established in 1983 is incomplete and that the situation is far more complex, including inversion layers at various altitudes and temporal changes on all time scales (Clancy et al., 2003; Drossart et al., 2007; Pätzold et al., 2007; Rengel et al., 2008; Sonnabend et al., 2008b). New self consistent general circulation models for the venusian atmosphere are currently under development (Lebonnois et al., 2010) and need to be validated against experimental data that span a broader range of altitudes.

The spacecraft data are limited by instrumental constraints and mission lifetime. Especially altitudes above 100 km are still poorly constrained in terms of key physical properties such as temperatures and winds. Complementary ground based observations can probe atmospheric regions not otherwise accessible remotely and can provide long-term coverage.

Original information on Venus atmospheric temperature profiles was gathered in the 1980s by the Pioneer Venus (PV) Probes, the PV Orbiter, and the Venera landers. In the model temperatures decrease with altitude from cloud top values of ~240 K to 170 K at 90 km altitude with an eventual increase to ~190 K at 120 km on the day side of Venus.

* Corresponding author.
*E-mail address:* samstag@ph1.uni-koeln.de (G. Sonnabend).

[1] Visiting Astronomer at the Infrared Telescope Facility, which is operated by the University of Hawaii under Cooperative Agreement no. NNX-08AE38A with the National Aeronautics and Space Administration, Science Mission Directorate, Planetary Astronomy Program.

0019-1035/$ - see front matter © 2011 Elsevier Inc. All rights reserved.
doi:10.1016/j.icarus.2011.07.015

From measurements of fully resolved molecular transition lines in planetary atmospheres physical parameters such as pressure, temperature, molecular abundance, and dynamical properties (i.e. wind velocities) of the atmosphere are retrieved from single line profiles (Kostiuk, 1994). In the case of Venus, temperatures can be measured directly by using emission lines of $CO_2$, the major constituent of the atmosphere, in the 9–10 μm spectral region. These non-thermal (non-LTE) emission lines originate from the upper mesosphere/lower thermosphere and are pumped by solar irradiation. At a pressure level of 0.15 Pa (corresponding to an altitude of 110 ± 10 km in current models (Lopez-Valverde et al., in press)) the probability of emitting a photon exceeds that of collisions between two $CO_2$ molecules within the natural lifetime of the meta-stable upper state of the 9.6 and 10.6 μm lasing bands of $CO_2$. On the other hand, the pumping only affects the vibrational temperatures of the emitting $CO_2$ gas and thus the rotational and kinetic temperatures are expected to be in equilibrium with the physical temperature of the atmosphere in that region. At these pressure levels pressure broadening of the $CO_2$ emission lines is insignificant and these lines are Doppler broadened Gaussian features whose half width is determined by the local kinetic temperature, qualifying these lines as direct probes for the physical temperature of the emitting gas. For more details on the non-LTE process, see Deming and Mumma (1983) and Lopez-Valverde et al. (in press).

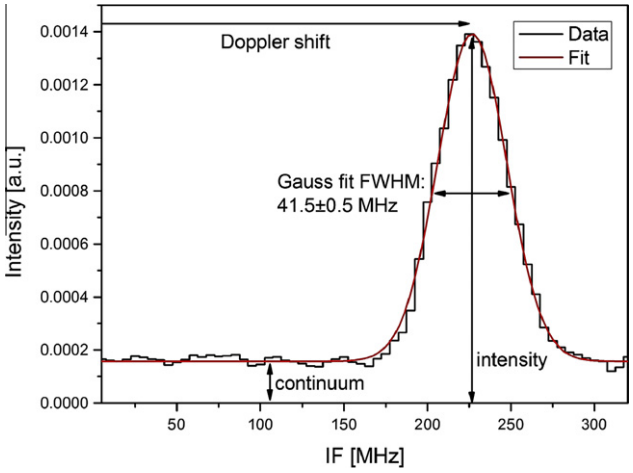


**Fig. 1.** Typical spectrum of an IRHS observation observed on January 4 1990 at Equator and 70° West of the central meridian longitude (CML). Shown is the measured emission core of the R8 line of the 10.4 μm band of $CO_2$. The spectral resolution is 5 MHz. IF (intermediate frequency) corresponds to the difference frequency with respect to the laser local oscillator and the frequency of the range of the tunable high resolution filterbank. The line is fitted by a Gaussian profile. The width of the Gaussian of 41.5 ± 0.5 MHz directly yields a temperature of 244 ± 5 K of the emitting gas via Eq. (1).

## 2. Infrared heterodyne observations from 1990 and 1991

Non-LTE emission in the 10 μm spectral region was detected on Venus by Betz et al. (1976) and further explored by Deming et al. (1983) using IR heterodyne spectroscopy. Since photons are emitted from the metastable state of $CO_2$ between molecular collisions, the only source of line-broadening in excess of the natural line width is Doppler shift due to the Maxwellian distribution of translational velocity in the gas. At Venus upper atmospheric temperatures, the Doppler width is of order 40 MHz. For transitions at ~10 μm wavelength ($1000\,cm^{-1} \approx 30\,THz$), spectral resolving power greater than $\nu/\Delta\nu 10^6$ is required to measure the line widths and directly probe the temperature in the non-LTE source region. The only remote spectroscopic technique with this capability is infrared heterodyne spectroscopy. Mid-IR heterodyne observations have proven to be a valuable tool for planetary astronomy since the 1970s and important results have been achieved on Mars, Venus, Saturn, Jupiter and Titan (Fast et al., 2006; Sonnabend et al., 2010; Kostiuk et al., 1996, 2001; Sornig et al., 2008).

### 2.1. Instrument and observations

The presented observations were acquired at the NASA Infrared Telescope Facility (IRTF, Mauna Kea, Hawaii, USA) on January 3–5 and February 4–5 1990 and August 9–11 and September 6–9 1991. The data have been previously analyzed only with regard to winds (Schmülling et al., 2000). A more detailed analysis of wind values and a comparison to current observations is currently in preparation and will be published elsewhere.

The pointing uncertainty was estimated to be ~1 arcsec. Seeing conditions varied from 1 to 2 arcsec. The angular diameter of the apparent disk of Venus varied from 51 to 58 arcsec compared to a field of view of 0.9 arcsec. Fig. 1 shows a typical spectrum of the observed R8 line of the 10.4 μm band of $CO_2$. The spectrum was observed on January 4 1990 at the equator and 70° West of the central meridian longitude (CML). The observations were targeted along the center of the illuminated crescent, as shown in Fig. 2. The observed positions are summarized in Table 1. Integration times for each individual spectrum was ~100 s.

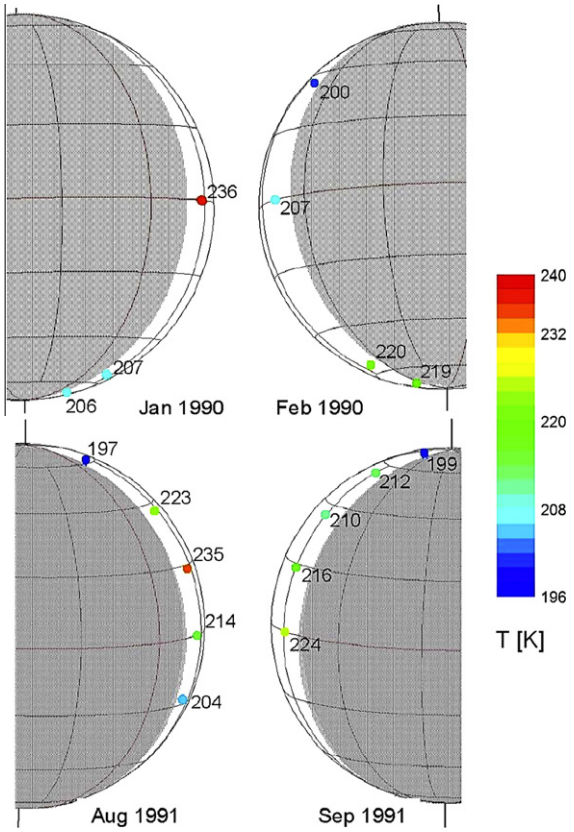


**Fig. 2.** All IRHS measurements of 1990 and 1991. The sizes of the colored dots relative to the size of the apparent disk of Venus correspond to the telescope FOV of 0.9 arcsecs.

The data were acquired using the NASA Goddard Infrared Heterodyne Spectrometer (IRHS). The infrared radiation from the source is mixed with the output of a Lamb-dip stabilized $CO_2$-laser local oscillator (LO) providing an accuracy of the LO frequency of a

**Table 1**
Retrieved values for the kinetic temperatures $T_{kin}$ observed with the IRHS in 1990 and 1991. Observed position shows latitude and offset to the CML. Venus local time is given as well. Quoted are 1-$\sigma$ uncertainties from the width parameter of the Gaussian fit to the spectra. Observations probe a pressure level of 0.15 Pa (corresponding to an altitude of 110 ± 10 km in current models (Lopez-Valverde et al., in press)).

| Observed position | $T_{kin}$ (K) | Local time |
|---|---|---|
| January 1990 | | |
| Equator/70°W | 236 ± 5 | 17:20 |
| 60S/70°W | 207 ± 5 | 17:20 |
| 80S/70°W | 206 ± 8 | 17:20 |
| February 1990 | | |
| 40N/70°E | 200 ± 5 | 6:40 |
| Equator/70°E | 207 ± 6 | 6:40 |
| 60S/70°E | 220 ± 3 | 6:40 |
| 80S/70°E | 219 ± 5 | 6:40 |
| August 1991 | | |
| 70N/80°W | 197 ± 6 | 16:40 |
| 40N/80°W | 223 ± 5 | 16:40 |
| 20N/80°W | 235 ± 13 | 16:40 |
| Equator/80°W | 214 ± 9 | 16:40 |
| 20S/80°W | 204 ± 6 | 16:40 |
| September 1991 | | |
| 80N/80°E | 199 ± 6 | 7:30 |
| 60N/68°E | 212 ± 9 | 6:40 |
| 40N/68°E | 210 ± 9 | 6:40 |
| 20N/68°E | 216 ± 6 | 6:40 |
| Equator/68°E | 224 ± 5 | 6:40 |

few hundred kHz and is then detected by a HgCdTe mixer–detector. Due to the non-linear detection characteristic of the mixer in addition to the signal generated by the individual frequencies of LO and sky signal the difference frequency of both signals is generated. The resulting so-called intermediate frequency (IF), which contains the full spectroscopic information of the source, is analyzed by an electronic filter bank of 25- and 5-MHz filter widths arranged in two arrays of 64 contiguous channels. The 5 MHz (high-resolution) filter bank can be tuned in frequency. Heterodyne instruments provide a diffraction limited field of view (FOV). At 10 μm wavelength, the FOV is 0.9 arcsec at a 3 m aperture telescope like the IRTF. The incoming radiation from the telescope is split by a dichroic mirror that reflects IR radiation into the spectrometer while transmitting visible light into an integrated optical guide system allowing active telescope tracking and accurate pointing. For more instrumental details see Kostiuk and Mumma (1983) and Goldstein et al. (1991).

Spectra were acquired using two instrumental beam paths, A and B. The beam was chopped between positions ON and OFF Venus (i.e. source vs. sky background). In order, to eliminate instrumental effects like standing waves originating in the spectrometer, the chop phase describing which beam was on-target and which was off was (so called "A" and "B" beam) alternated, a technique known in radio astronomy as "double beamswitch". Data were then analyzed by combining AB pairs. Occasional calibration measurements were obtained by chopping between a reference blackbody source at 1000 °C vs. room temperature. At ~270 K, thermal emission from the room is essentially negligible in comparison to the blackbody source. For more details on IR heterodyne observing strategies and instruments see Schmülling et al. (1998), Goldstein (1989), Mumma et al. (1982), Kostiuk and Mumma (1983), and Sonnabend et al. (2008a).

### 2.2. Data reductions and results

To minimize line broadening due to the changes of the radial velocity between the observer and Venus during observations, individual spectra were shifted appropriately to a common radial velocity accounting for the varying Doppler shift before co-adding to generate a resultant spectrum.

The observed emission line profiles have Gaussian line shapes as the pressure at the emitting altitude is sufficiently low to neglect pressure broadening.

The kinetic temperature of the gas is retrieved from the width of the observed emission line, in which the temperature is directly proportional to the square of the line width according to the standard results of statistical mechanics for a gas in thermal equilibrium,

$$\Delta v_D = \frac{v_0}{c}\sqrt{\frac{8k_B T_{kin}\ln(2)}{m}}. \quad (1)$$

The full width at half-maximum (FWHM) of the observed Doppler-broadened line is $\Delta v_D$, $v_0$ is the rest frequency of the observed transition, $m$ is the molecular mass of $CO_2$, $T_{kin}$ is the kinetic temperature in Kelvin, and the proportionality constants $c$ and $k_B$ are the speed of light and the Boltzmann constant, respectively (Bernath, 2005).

The results are given in Table 1, ranging from a minimum of 197 ± 6 K at 70°N to a maximum of 236 ± 5 K on the equator, both on the western (dusk) limb. As stated above a pressure level of 0.15 Pa is probed.

Table 1 gives the 1-sigma formal statistical uncertainties derived from an analysis of the curvature of the phase space around the optimal solution to fitting the spectrum, in which the axes of the phase space are the free parameters of the fit. The fitted parameters are the line width, line intensity, baseline (pedestal) intensity, and the Doppler shift of the emission line relative to the laser local oscillator frequency. The uncertainty analysis incorporates covariances between the fitted parameters which dominate the precision of the temperature retrieval. Sources of systematical errors are LO-laser instabilities and the possible effect of underlying absorption features of the measured line. These error sources are discussed in detail below.

The frequency stability of the local oscillator was determined to be better than 0.1 MHz due to the employed Lamb-dip stabilization (Goldstein, 1989). Compared to the line width of the emission features of ~40 MHz the broadening due to laser instabilities is negligible.

Close inspection of the thermal continuum emission in Fig. 1 reveals a shallow pressure-broadened absorption feature centered on the emission line, due to the shallow temperature lapse above the cloud tops before reaching the temperature minimum of the mesopause. The shallow temperature increase above this altitude should result in a thermospheric emission line due to thermal processes. Previous analyses Deming and Mumma (1983) have shown that this emission component is negligible compared to the non-LTE emission. The thermal emission and absorption components thus have a trivial influence on the retrieved line widths. The width, Doppler shift, and intensity of the non-LTE lines can be evaluated accurately without requiring detailed radiative-transfer analysis of the complete atmosphere.

The results from three observations, January 1990 and both observing runs in 1991, show a latitudinal dependence of temperatures decreasing from low to high latitudes with values reaching 224–236 K close to the equator and then decreasing to 197–199 K at 70–80° latitude (see Fig. 3). Typical retrieval errors are below 10 K. Although the temperatures generally decrease from equatorial regions to higher latitudes, February 1990 is the exception showing temperatures of ~220 K near 60° and 80° southern latitudes while the temperature at the equator only reaches 207 K. In addition, in all cases the variability of the measured temperatures at a given latitude is quite high between the different observing times.

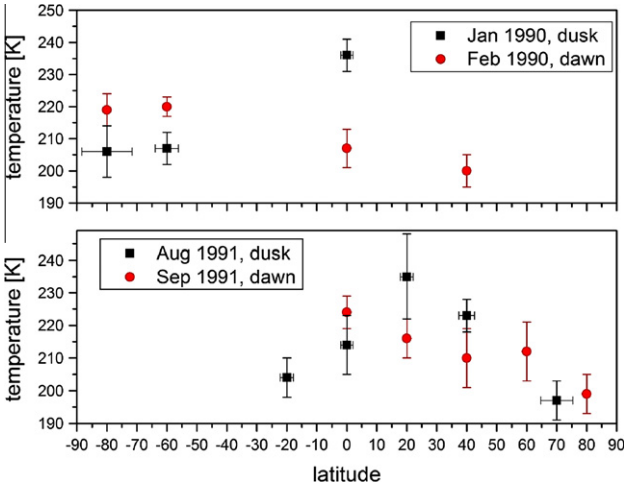


**Fig. 3.** Temperatures vs. latitude for the four IRHS runs. Black indicates dusk, red dawn observations. In January 1990 and both runs in 1991 the warmest temperatures are seen at low latitudes with a decrease towards the poles. Only in the February 1990 case the observed values increase to higher latitudes with unusual high temperatures near the South Pole.

### 2.3. Discussion

In the following we evaluate the statistical confidence of differences between dusk and dawn terminator as well as between low and high latitudes. The differences were calculated by using the individual observations and their uncertainties or the variance weighted averages and the corresponding uncertainties in cases where multiple measurements were available. An overview of the used values is given in Table 2.

When we compare the dusk and dawn temperature retrievals for 1990 and 1991 we find that with high statistical confidence of 2 to 3-$\sigma$ the dusk region in 1990 was warmer than the dawn side by 13–29 K for both polar and equatorial regions, respectively, while in 1991 no statistical confidence of a temperature difference was found.

Comparing near-equator to circumpolar regions, we find that in January 1990, equator is 29 K warmer than South circumpolar region yielding a 4.5-$\sigma$ confidence. In August 1991 near-equator is 14 K warmer than North circumpolar (2.7-$\sigma$ confidence) and September 1991, equator is 21 K warmer than North circumpolar (3-$\sigma$). Only in February 1990, equator is 13 K cooler than South circumpolar resulting in a 2-$\sigma$ confidence. Therefore, three out of four observations show decreasing temperatures towards the poles.

**Table 2**
Calculated contrasts for dusk-to-dawn as well as equatorial-to-polar region comparison. In cases where multiple observations are available we used a variance-weighted average. For the polar region we included all values above 60° latitude; the equatorial region includes values within ±20° latitude.

| Location | January 1990 dusk | February 1990 dawn | Dusk-to-dawn contrast |
|---|---|---|---|
| Equatorial region | 236 ± 5 | 207 ± 6 | 29 ± 8 |
| Polar region | 206 ± 5 | 219 ± 3 | −13 ± 5 |
| Equator-to-pole contrast | 29 ± 7 | −13 ± 7 | |
| | August 1991 dusk | September 1991 dawn | Dusk-to-dawn |
| Equatorial region | 218 ± 5 | 218 ± 10 | 0 ± 11 |
| Polar region | 204 ± 5 | 197 ± 6 | 7 ± 8 |
| Equator-to-pole contrast | 14 ± 5 | 21 ± 7 | |

The reason for this behavior is not obvious but could be due to the dynamical properties of the upper mesosphere. The altitude region of ~110 km is dominated by the subsolar-to-antisolar (SS–AS) flow generated by the solar insolation on the day side. Fairly stable cross terminator wind speeds of 100–150 m/s have been measured by the same technique used for the temperature observations presented here (Goldstein et al., 1991; Sornig et al., 2009). Due to the strong winds warm gas from regions closer to the subsolar point is transported towards the terminator thus leveling the dusk and dawn contrast. However, a weaker and more variable zonal wind component of 15–45 m/s has been detected, too (Goldstein et al., 1991; Sornig et al., 2009, 2012), which might explain the remaining variability in the dusk to dawn temperature contrast. Dynamics might also explain the observed temperature difference between the equatorial regions and the polar regions. In first order approximation, the SS–AS flow is assumed to be spherical symmetric since it is caused by insolation which can be described by the solar zenith angle (SZA) (Goldstein et al., 1991). Sornig et al. (2009) found, however, that the cross-terminator flow decreases strongly with latitude polewards of 60°. At this point, we can only speculate if the polar vortex could have an influence, such as shifting the non-LTE emitting region downward. Heating due to subsiding gas circulating towards the pole may explain the warmer temperature at high latitude in February 1990. This can be driven by meridional or subsolar-to-antisolar wind aided by effects at 110 km altitude driven from below by a variable and active polar vortex (Titov et al., 2008; Piccioni et al., 2009), which is associated with rapid down-welling and thus adiabatic heating. No additional explanation than the changing nature of the vortex can be given at this point to why this effect only appeared in the February 1990 data.

Along the subsolar meridian the insolation at different latitudes described by the solar zenith angle (SZA) could cause a temperature decrease from low to high latitudes, since the gas at different latitudes is exposed to radiation for long periods of time. However, in the presented observing geometries the SZA varies only between 79° and 87°. Still the length of insolation could easily be responsible for a dusk to dawn temperature gradient. However, since this was not seen in 1991 it cannot be the dominant influence. The same is true for the influence of slight differences in Venus' distance from the Sun and possible "seasonal" effects due to the small variations in the latitude of the subsolar point.

All values observed in 1990/1991 exceed the predicted value for that altitude by VIRA of 178 K (Keating et al., 1985).

## 3. Comparison of observations of mesospheric temperatures using various techniques

In the next section we compare the results from the 1990/1991 IRHS observations presented above to other temperature measurements in the targeted region of the Venus atmosphere, namely IR heterodyne observations using the Cologne Tuneable Heterodyne Infrared Spectrometer (THIS), sub-mm results observed at the James-Clerk-Maxwell-Telescope on Mauna Kea, HI, and very recent rotational temperature retrievals using data from the SOIR instrument on board VEX.

### 3.1. Comparison to infrared heterodyne observations from 2009

In 2009 two observing campaigns were performed in March/April using the Cologne Tuneable Heterodyne Infrared Spectrometer (THIS) at the McMath–Pierce Solar Observatory on Kitt Peak, Az (Sonnabend et al., 2010). These runs were very similarly scheduled around inferior conjunction as the four observing runs with the IRHS instrument in 1990/1991. The IRHS runs were scheduled 2 weeks before and after inferior conjunction and IRHS observed

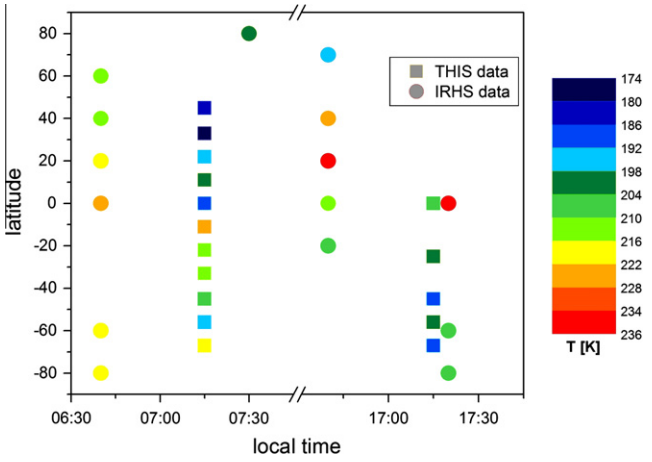


**Fig. 4.** Comparison of IRHS and THIS data. Plotted are the observed IRHS latitudes vs. local time. THIS data is adopted from Sonnabend et al. (2010). The color codes for the symbols represent the observed temperatures. IRHS was observing higher temperatures than THIS. See text for discussion.

in the middle of the illuminated crescent of the disc of Venus. The observations with THIS were scheduled 1 week before and after inferior conjunction and observations were performed at the limb. This results in observation closer to the terminator for IRHS runs compared to THIS data. In general, THIS observed lower temperatures than IRHS. In Fig. 4 all observed IRHS latitudes with respect to Venus local time are presented. THIS data is adopted from Sonnabend et al. (2010). The uncertainties for individual values are below 10 K, see Sonnabend et al. (2010) for details. The color[2] codes represents the measured temperatures. The average over all values is 214 ± 2 K for the IRHS data and 200 ± 2 K for the THIS data.

The statistical significance for a global temperature change between 2009 and 1990/1991 is larger than between 1990 an 1991 data. All short term variations are canceled out due to the averaging over a range of dates, times and latitudes. Therefore we think that in addition to the intrinsic dynamical short term variability other effects play a role. An important aspect in understanding the reason for THIS seeing lower temperatures than IRHS might be the solar activity. It is well proven that temperatures in the higher thermosphere (around 200 km) do significantly differ between solar activity minimum and maximum. Kliore and Mullen (1990) and Kliore (1989) report for 160–170 km altitude a neutral atmosphere temperature shift from 250 K during solar minimum to 300 K during solar maximum. Observations with IRHS in 1990 and 1991 were performed near a solar maximum. In contrast, 2009 was a year with exceptionally low solar activity, even for a solar minimum.

A systematic instrumental effect like a broadening of the observed lines due to LO instability cannot be ruled out completely however it is unlikely due to the Lamb-dip stabilization of the $CO_2$-laser used in IRHS. It is unlikely that using different $CO_2$ transition lines would have any effect like probing different altitudes and yielding unequal temperatures. This effect, however, was determined to be negligible based on recent modeling results (Lopez-Valverde et al., in press). Also the difference in the FOVs of the used telescopes, 0.9 arcsec for IRHS at the IRTF and 1.7 arcsec for THIS at the McMath–Pierce, cannot be responsible for the observed differences. A larger FOV could lead to an averaging effect, flattening out the maximum and minimum values but it is unlikely that it would lead to a generally higher or lower temperature retrieval.

[2] For interpretation of color in Figs. 1–6, the reader is referred to the web version of this article.

In order to prove a correlation with solar activity, data of other solar cycle phases are needed. More Venus data from IRHS observations exist and will be analyzed in the near future. IRHS was decommissioned in 1999 but additional observations with the successor instrument HIPWAC as well as THIS are planned for the upcoming years as the solar activity is expected to increase again in the future.

A direct connection to solar activity however is in disagreement with earlier observations from 2007 and 2009 presented in Sonnabend et al. (2008b). In those data we found warmer temperatures in 2007 compared to 2009. The solar cycle was close to minimum activity in both cases. It has to be noted though, that in 2007 the instrument HIPWAC was used, which so far lacks the precise frequency control of lamb dip stabilized IRHS or the reference gas measurements in THIS. Thus an instrumental effect leading to higher values cannot be ruled out completely. In addition, those data were acquired only at the equator and over the course of a few hours. The averaging effect described above therefore does not apply so that the observed higher temperatures could well be in the range of the already mentioned short term regime.

### 3.2. Comparison to sub-mm observations

In the following section we compare temperature retrievals from IR heterodyne observations with IRHS in 1990/1991 and THIS in 2009 to sub-mm observations performed between 2001 and 2009 by Clancy et al. (2012).

In Fig. 5 retrieved sub-mm temperature profiles from day- and night side observations under different solar activity conditions (solar maximum 2000–2002, solar minimum 2007–2009) (Clancy et al., 2012) are compared to IR heterodyne values measured with IRHS in 1990/1991 (solar maximum) and THIS in 2009 (solar minimum) (Sonnabend et al., 2010).

For the IR heterodyne observations we generated three averaged values. Two points include all values observed close to the terminator (and thus the night side) at a SZA > 85° for both, THIS in March/April 2009 and IRHS in 1990/1991, respectively. The third point represents an average of all day side equator observations performed with THIS in June 2009. The averaged sub-mm

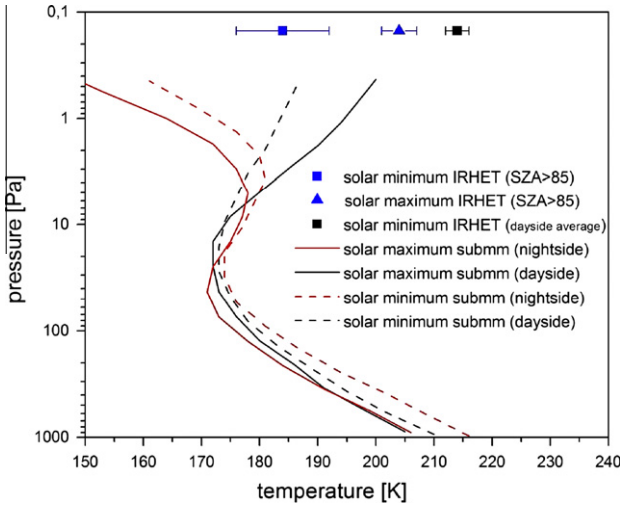


**Fig. 5.** Comparison of IR heterodyne and sub-mm temperatures. Shown are averaged profiles from Clancy et al. (2012) for different solar activity conditions (solar maximum 2000–2002, solar minimum 2007–2009). The 1-$\sigma$ precision at the top of the profile (0.4 Pa, 106 km) is ~±5 K. In addition, averaged values for IR heterodyne observations are given for SZA > 85° for different solar activities in 1990/91 and 2009 (in blue) as well as a day side average for 2009 observations (in black).

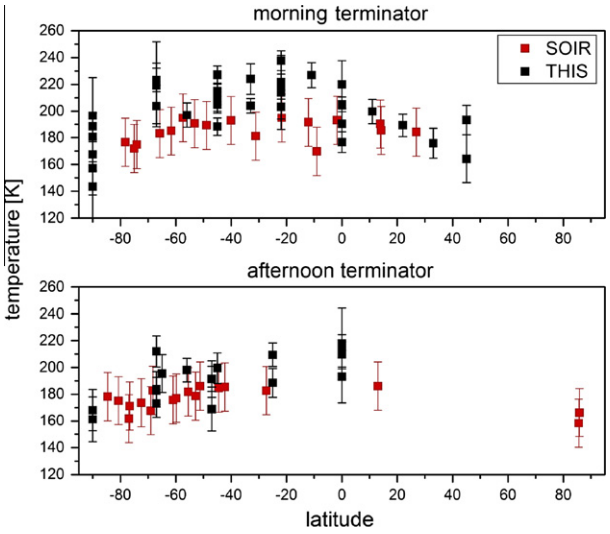


**Fig. 6.** Comparison of IR heterodyne and SOIR temperatures from March 2009 (IR heterodyne) and January 2009 to February 2010 (SOIR, occultation seasons 10–13). Shown for SOIR are retrieved values for 110 ± 3 km. Values are separated for morning and afternoon terminator. Error bars for SOIR are estimated to be in the order of 15 K, THIS uncertainties are usually on the order of 10 K with some exceptions due to lower signal-to-noise of the acquired data. Since SOIR observes at the terminator we only include IR heterodyne observations within 1.5 h local time around the terminator.

retrievals end at an altitude of ~106 km where the 1-$\sigma$ precision is ~±5 K and thus do not reach the probing altitude of the IR heterodyne observations of 110 km but a continuous increase in the temperature profile is expected by the VIRA model. As can be seen, even the high SZA values from the IR heterodyne campaigns differ from the night side sub-mm profiles due to the effect of the extended FOV of the sub-mm beam (~14″ compared to 1–2″ in the IR). However, for the day side sub-mm profiles as well as for the high SZA IR heterodyne observations the retrieved temperatures are significantly higher for the solar maximum case as for the solar minimum. In addition, the day side average value for the 2009 IR heterodyne observations agrees quite well with the sub-mm profile since close to maximum elongation the sub-mm FOV samples the full day side of the planet. Detailed comparison to sub-mm observations would require beam integrated modeling to account for the differences in FOV between sub-mm and IR.

### 3.3. Comparison to SOIR profiles

Recently, the team of the solar occultation IR instrument (SOIR) on board VEX reported retrieval of rotational temperatures from analysis of $CO_2$ features between 2.2 and 4.4 μm wavelength (Mahieux et al., 2010). Since SOIR operates in solar occultation mode for these retrievals only temperatures close to the terminator (~6 and 18 h local time) are detected (except at very high latitudes). Typical profiles range from 80 to 170 km in altitude. The retrieved temperatures at 110 km, the altitude of the IR heterodyne measurements, range from 160 to 190 K (Mahieux et al., in preparation). This is very similar to the range of temperatures from the IR heterodyne observations presented above. A more detailed comparison of the latitudinal distribution is presented in Fig. 6. Included there are values observed with SOIR between February and June 2009 (occultation season 10 and 11) and THIS in March/April 2009 (Sonnabend et al., 2010) limited to a local time range of 1.5 h from the terminator into the day side for the morning terminator (6h local time) and the afternoon terminator (18h local time). In general, the IR heterodyne values are warmer than the SOIR values by about 15 K on average. This however can be easily explained by the differences in the FOV and the assumption that the day side is warmer than the night side. Even if we would only use IR heterodyne values centered at the terminator (SZA = 90) we would see a contribution from lower SZAs due to the extended FOV of the ground based observations. The much smaller FOV of the SOIR instrument compared to ground based IR heterodyne observations will certainly allow a more detailed insight to the small scale variability of mesospheric temperatures. Also it should be noted, that while the altitude information for the SOIR observations is only dependent on the observing geometry it has to be derived for the IR heterodyne measurements from a temperature profile that might be deficient. The key variable here is the pressure of the gas where non-LTE conditions occur. Coordinated observations and use of updated temperature profiles will lead to an improved understanding and cross-validation in the future.

## 4. Conclusion

Measurements with IR heterodyne spectroscopy demonstrate a high variability of Venus' upper mesospheric/lower thermospheric temperatures. Short-term variations of up to 30 K at low latitudes within a few (Earth-)days were recorded. Close to the poles temperatures tend to be more stable with variability of up to 15 K. This is in agreement with other observations performed using sub-mm Earth-based and near-IR spectroscopy. This indicates a much more turbulent atmosphere at altitudes around 100–120 km than thought before. A reason for such turbulence can be the transition between the two global wind patterns: the retrograde zonal superrotation (RZS) in the troposphere and lower mesosphere, and the SS–AS flow in the thermosphere are basically different atmospheric regions. At some altitude the RZS has to turn over to the SS–AS flow, which is aligned in the opposite direction for the morning terminator hemisphere. Both wind patterns are expected to reach wind speeds in the order of 100 m/s. Therefore it would not be surprising if massive turbulences occur in the transition zone, giving rise to the observed temperature variations. The observed variability between the campaigns has to be studied in more detail before valid conclusions can be drawn.

The temperature retrievals from different observing techniques for the given altitude of 110 km altitude agree quite well if the limitations of observational constraints are taken into account. Differences to the sub-mm values can be explained by the different FOV while disagreement to the SOIR values is due to FOV and limitation to terminator measurements. The comparison to space observations from SOIR are promising and a good example for the complementarity of ground based and space based observations.

The observed high temperature values disagree with the VIRA atmosphere model as presented by Keating et al. (1985). However, the authors of that work state already that the simple division into day and night time profiles without latitudinal or local time dependence for the altitude range of 100–150 km is due to the lack of data and that reality might be far more complex. Thus, a new reference atmosphere model is urgently needed.

IR heterodyne observations of Venus go back to 1980. However, most data have only been analyzed for winds but not for temperatures. Additional data are currently re-analyzed and will provide a long term study of the temperatures in the Venus mesosphere only possible by ground based observations.

## Acknowledgments

Research at the NASA Infrared Telescope Facility was supported by the National Aeronautics and Space Administration Planetary Astronomy Program. This work was supported by the Deutsche

Forschungsgemeinschaft (DFG) through Grant SO879/1-2. We would like to thank the SOIR team, especially Jean-Loup Bertaux, PI of the instrument, and Ann Carine Vandaele, group leader at the Belgian Institute for Space Aeronomy, Brussels. The research program was supported by the Belgian Federal Science Policy Office and the European Space Agency (ESA, PRODEX program, contracts C90268, 90113, and 17645).

## References

Bernath, P., 2005. Spectra of Atoms and Molecules. Oxford University Press.
Betz, A.L., Johnson, M.A., McLaren, R.A., Sutton, E.C., 1976. Heterodyne detection of $CO_2$ emission lines and wind velocities in the atmosphere of Venus. Astrophys. J. 208, L141–L144.
Clancy, R.T., Sandor, B.J., Moriarty-Schieven, G.H., 2003. Observational definition of the Venus mesopause: Vertical structure, diurnal variation, and temporal instability. Icarus 161, 1–16.
Clancy, R.T., Sandor, B.J., Moriarty-Schieven, G.H., 2012. Thermal structure and CO distribution for the Venus mesosphere/lower thermosphere: 2001–2009 Inferior conjunction sub-millimeter CO absorption line observations. Icarus 217 (2), 779–793.
Deming, D., Mumma, M.J., 1983. Modeling of the 10-micron natural laser emission from the mesospheres of Mars and Venus. Icarus 55, 356–368.
Deming, D., Espenak, F., Jennings, D., Kostiuk, T., Mumma, M., Zipoy, D., 1983. Observations of the 10-micron natural laser emission from the mesospheres of Mars and Venus. Icarus 55, 347–355.
Drossart, P. et al., 2007. A dynamic upper atmosphere of Venus as revealed by VIRTIS on Venus EXpress. Nature 450, 641–645.
Fast, K., Kostiuk, T., Hewagama, T., A'Hearn, M.F., Livengood, T.A., Lebonnois, S., Lefèvre, F., 2006. Ozone abundance on Mars from infrared heterodyne spectra. Icarus 183, 396–402.
Goldstein, J.J., 1989. Absolute Wind Measurements in the Lower Thermosphere of Venus Using Infrared Heterodyne Spectroscopy. Thesis, University of Pennsylvania, Philadelphia.
Goldstein, J.J., Mumma, M.J., Kostiuk, T., Deming, D., Espenak, F., Zipoy, D., 1991. Absolute wind velocities in the lower thermosphere of Venus using infrared heterodyne spectroscopy. Icarus 94, 45–63.
Keating, G.M., Bertaux, J.L., Bougher, S.W., Dickinson, R.E., Cravens, T.E., Hedin, A.E., 1985. Models of Venus neutral upper atmosphere – Structure and composition. Adv. Space Res. 5, 117–171.
Kliore, A.J., 1989. Solar cycle changes in Venus upper atmosphere temperatures. Bull. Am. Astron. Soc. 21, 925.
Kliore, A.J., Mullen, L.F., 1990. Solar-cycle changes in the thermal structure of the Venus day side ionosphere. Adv. Space Res. 10, 15–29.
Kostiuk, T., 1994. Physics and chemistry of upper atmospheres of planets from infrared observations. Infrared Phys. Technol. 35, 243–266.
Kostiuk, T., Mumma, M., 1983. Remote sensing by IR heterodyne spectroscopy. Appl. Opt/ 22, 2644–2654.
Kostiuk, T., Buhl, D., Espenak, F., Romani, P., Bjoraker, G., Fast, K., Livengood, T., Zipoy, D., 1996. Stratospheric Ammonia on Jupiter after the SL9 Collision. Icarus 121, 431–441.
Kostiuk, T. et al., 2001. Direct measurement of winds of Titan. J. Geophys. Res. Lett. 28, 2361–2364.
Lebonnois, S., Hourdin, F., Eymet, V., Crespin, A., Fournier, R., Forget, F., 2010. Superrotation of Venus' atmosphere analyzed with a full general circulation model. J. Geophys. Res. 115, E06006. doi:10.1029/2009JE003458.
Lopez-Valverde, M.A., Sonnabend, G., Sornig, M., Kroetz, P., in press. Modelling the atmospheric $CO_2$ 10-μm non-thermal emission in Mars and Venus at high spectral resolution. Planet. Space Sci. doi:10.1016/j.pss.2010.11.011.
Mahieux, A. et al., 2010. Densities and temperatures in the Venus mesosphere and lower thermosphere retrieved from SOIR on board Venus EXpress. Part I. Retrieval technique. J. Geophys. Res. 115, E12014.
Mahieux, A., Vandaele, A.C., Drummond, R., Robert, S., Wilquet, V., Bertaux, J.L., in preparation. Densities and temperatures in the Venus mesosphere and lower thermosphere retrieved from SOIR on board Venus EXpress. Part II. $CO_2$ densities and temperatures. J. Geophys. Res.
Mumma, M.J., Kostiuk, T., Buhl, D., Chin, G., Zipoy, D., 1982. Infrared heterodyne spectroscopy. Opt. Eng. 21, 313–319.
Pätzold, M. et al., 2007. The structure of Venus' middle atmosphere and ionosphere. Nature 450, 657–660.
Piccioni, G., Politi, R., Drossart, P., 2009. The many faces of the Venus' polar vortex. In: European Planetary Science Congress 2010, p. 480.
Rengel, M., Hartogh, P., Jarchow, C., 2008. Mesospheric vertical thermal structure and winds on Venus from HHSMT CO spectral-line observations. Planet. Space Sci. 56, 1368–1384.
Schmülling, F., Klumb, B., Harter, M., Schieder, R., Vowinkel, B., Winnewisser, G., 1998. High-sensitivity mid-Infrared Heterodyne Spectrometer with a tunable diode laser as a local oscillator. Appl. Opt. 37, 5771–5776.
Schmülling, F., Goldstein, J., Kostiuk, T., Hewagama, T., Zipoy, D., 2000. High precision wind measurements in the upper Venus atmosphere. Bull. Am. Astron. Soc. 32, 1121.
Seiff, A., Schofield, J.T., Kliore, A.J., Taylor, F.W., Limaye, S.S., 1985. Models of the structure of the atmosphere of Venus from the surface to 100 kilometers altitude. Adv. Space Res. 5, 3–58.
Sonnabend, G., Sornig, M., Krötz, P., Stupar, D., Schieder, R., 2008a. Ultra high spectral resolution observations of planetary atmospheres using the Cologne Tuneable Heterodyne Infrared Spectrometer. J. Quant. Spectrosc. Res. Trans. 109, 1016–1029.
Sonnabend, G., Sornig, M., Schieder, R., Kostiuk, T., Delgado, J., 2008b. Temperatures in Venus upper atmosphere from mid-infrared heterodyne spectroscopy of $CO_2$ around 10 μm wavelength. Planet. Space Sci. 56, 1407–1413.
Sonnabend, G., Kroetz, P., Sornig, M., Stupar, D., 2010. Direct observations of Venus upper mesospheric temperatures from ground based spectroscopy of $CO_2$. J. Geophys. Res. Lett. 37, L11102.
Sornig, M. et al., 2008. Venus upper atmosphere winds from ground-based heterodyne spectroscopy of $CO_2$ at 10 μm wavelength. Planet. Space Sci. 56, 1399–1406.
Sornig, M. et al., 2009. Dynamics of Venus upper atmosphere from infrared heterodyne spectroscopy of $CO_2$. AAS/Division for Planetary Sciences Meeting 41. Abstracts #63.03.
Sornig, M., Sonnabend, G., Kroetz, P.J., Stupar, D., 2012. Direct wind measurements from November 2007 in Venus' upper atmosphere using ground-based heterodyne spectroscopy of $CO_2$ at 10 micron wavelength. Icarus 217 (2), 863–874.
Titov, D.V. et al., 2008. Atmospheric structure and dynamics as the cause of ultraviolet markings in the clouds of Venus. Nature 456, 620–623.